Food Anal. Methods (2016) 9:3080–3086
DOI 10.1007/s12161-016-0499-1

An Improved Chemiluminescence Immunoassay for the Ultrasensitive Detection of Aflatoxin B_1

Junfeng Li[1] · **Xiangyi Fang**[1] · **Yucong Yang**[2] · **Xiaoli Cheng**[2] · **Peng Tang**[1]

Received: 11 November 2015 / Accepted: 28 March 2016 / Published online: 4 April 2016

Abstract An indirect competitive chemiluminescence (CL) immunoassay based on Fe_3O_4@SiO_2@Au magnetic nanoparticles (Au-SCMPs) has been optimized and developed for the detection of aflatoxin B_1 (AFB_1). To improve the detection sensitivity and efficiency, this method combines 2′,6′-dimethylcarbonylphenyl-10-sulfopropyl acridinium-9-carboxylate 4′-NHS ester (NSP-DMAE-NHS) as a new kind of high efficient luminescence reagent with a simplified separation procedure based on the optimized Au-SCMPs. Superparamagnetic nanoparticles were coated with different sizes of Au colloids (18, 30, and 50 nm), and their capacities in immobilization of bovine serum albumin (BSA) were investigated. The BSA-AFB_1 conjugate (BSA-AFB_1) was immobilized on the optimized Au-SCMPs and competed with the free AFB_1 for specially binding the NSP-DAME-NHS-labeled anti-AFB_1 antibody (mAb-AFB_1). After the indirect competitive immunoreactions and magnetic separation, the CL of the nanoparticles was measured by a homemade luminescent measurement system. Under the optimum conditions, the IC_{50} value was 0.07 ng mL^{-1} and the limit of detection (LOD) of AFB_1 was 0.01 ng mL^{-1}, respectively. The result shows a much lower IC_{50} and LOD than that typically achieved by ELISA. This proposed immunoassay method was rapid, low-cost, and suitable for the detection of AFB_1.

Keywords Chemiluminescence immunoassays · Aflatoxin B_1 · Acridinium ester · Fe_3O_4@SiO_2@Au magnetic nanocomposites

Introduction

In recent years, magnetic nanoparticles are attracting great interest due to their promising application in many areas such as drug delivery, food and food industry, magnetic resonance imaging, and environmental remediation (Blasco and Picó 2011; Edelman and Warach 1993; Pankhurst et al. 2003; Zhang et al. 2010). To overcome the problems of toxicity and agglomeration limiting the application of magnetic nanoparticles in biological field, magnetic nanoparticles were often coated with various kinds of shells (Deng et al. 2005). The silica shell is one of the most appropriate layers for its good chemical stability, excellent biocompatibility, and water dispersibility (Ahangaran et al. 2013; Hui et al. 2011). Also, silica shell facilitates further coupling interaction with some guest molecules because of the abundant amounts of functional groups which is a great improvement for magnetic nanoparticles (Mojić et al. 2012). As we know, gold has been considered as one of the best materials because of its special characteristics such as reliable chemical stability, biocompatibility, and versatility in surface modification (Ackerson et al. 2006; Lim et al. 2008). Gold nanoparticles can provide a high density and stable immobilization of proteins while retaining their bioactivity. However, the problematic way of isolation limited the application of gold nanoparticles in immunoassays. Up to now, various methods have been developed to synthesize Fe_3O_4@SiO_2@Au (Au-SCMPs) magnetic nanoparticles for the immobilization and separation of protein. Au-

Electronic supplementary material The online version of this article (doi:10.1007/s12161-016-0499-1) contains supplementary material, which is available to authorized users.

✉ Xiangyi Fang
577997201@qq.com

[1] Physics Department, School of Science, Xi'an Jiaotong University, Xi'an, People's Republic of China

[2] Department of Clinical Laboratory, The First Affiliated Hospital of Medical College, Xi'an Jiaotong University, Xi'an, People's Republic of China

SCMPs with unique magnetic responsivity and excellent stability perform easy binding of proteins and its recovery which is a great achievement in biological applications.

Aflatoxin B_1 (AFB_1) is one of the most toxic, carcinogenic, and immunosuppressive mycotoxins which are mainly produced by *Aspergillus* in hot-humid area. In 1993, AFB_1 was designated as a group I carcinogen by the International Agency for Research on Cancer (IARC). AFB_1 is a very stable coumarin compound and usually contaminates agricultural commodities, such as peanuts, corn, and soybeans, which is an important problem all through (Xiulan et al. 2005). Many countries have specially established regulations to avoid overexposure of humans and animals to AFB_1 (Ren et al. 2014). The European commission has set very strict rules that the maximum permissible level for AFB_1 was 2 ppb or 6.4 nM in peanuts, tree nuts, milk, dried fruits, and all cereals (Castillo et al. 2015; Ren et al. 2014). Hence, the detection of AFB_1 is very important for food security. Up to now, various analytical methods have been developed for the detection of AFB1 such as enzyme-linked immunosorbent assay (ELISA), radioimmunoassay (RIA), and high-performance liquid chromatography (HPLC) (Herzallah 2009; Kolosova et al. 2006; Korde et al. 2003). However, most of the reported methods are laborious, instable, time-consuming, and requiring expensive equipment, materials, and maintenance. Therefore, searching analytical methods for the detection of AFB_1 that are simultaneously rapid, low-cost, and highly sensitive remains a challenge.

Chemiluminescence (CL) assay has been widely recognized as a promising analytical method in many fields such as immunoassays, pharmaceutical analysis, food analysis, and DNA probe-based assay (Bronstein et al. 1989; Mervartová et al. 2007; Navas and Jimenez 1996; Zhang et al. 2008). CL assay usually involves the oxidation of a suitable substrate (or analyte) to produce an excited species, which emits light (ultraviolet, visible, or infrared) upon relaxation to ground state (Iranifam et al. 2013). CL assay possesses the advantages of an acceptable sensitivity, inexpensive instrumentation, and wide dynamic range. However, there are still some drawbacks existed in CL assay such as the poor selectivity and the relativity low emission intensity which greatly influence the sensitivity of CL assay. During recent years, much effort has been made to catalyze redox CL reactions, providing enhanced CL emission (Bronstein et al. 1989; Mervartová et al. 2007; Navas and Jimenez 1996; Sorouraddin et al. 2008). 2′,6-Dimethylcarbonylphenyl-10-sulfopropyl acridinium-9-carboxylate 4′-NHS ester (NSP-DMAE-NHS) is a new kind of highly efficient chemiluminescent reagent which could emit light in less than 2 s and allow full automation. It is much more effective and easier than traditional chemiluminescent reagents such as luminal (Yang et al. 2009). On the other hand, Au-coated magnetic nanoparticles have shown great potential in CLIA for signal enhancement and protein immobilization (Bi et al. 2009; Pingarrón et al. 2008). Au-coated magnetic nanoparticles which possess high specific surface area will provide a high density of biomolecule immobilization. Moreover, they can also be easily separated from sample matrix retaining the biochemical activity of biomolecule such as proteins and DNA.

In this paper, indirect competitive chemiluminescent immunoassay based on the optimized Au-SCMPs for the ultrasensitive detection AFB_1 was first reported. The citrate-coated gold colloids with different size range self-assemble onto amine-SCMPs through attractive electrostatic interactions and their performance in immobilization of proteins were compared. The BSA-AFB_1 conjugate was immobilized on the optimized Au-SCMPs through the gold colloid adsorption, which could compete with the free AFB_1 in target analyte for binding to the NSP-DAME-NHS-labeled anti-AFB_1 antibody (mAb-AFB_1). The labeled mAb-AFB_1 bound to Au-SCMPs was then performed as chemiluminescence substrate induced by NaOH and H_2O_2 to yield different intensity of emitting light that corresponded to the level of AFB_1 analyses. The principle of CL detection based on Au-SCMPs is schematically shown in Fig. 1.

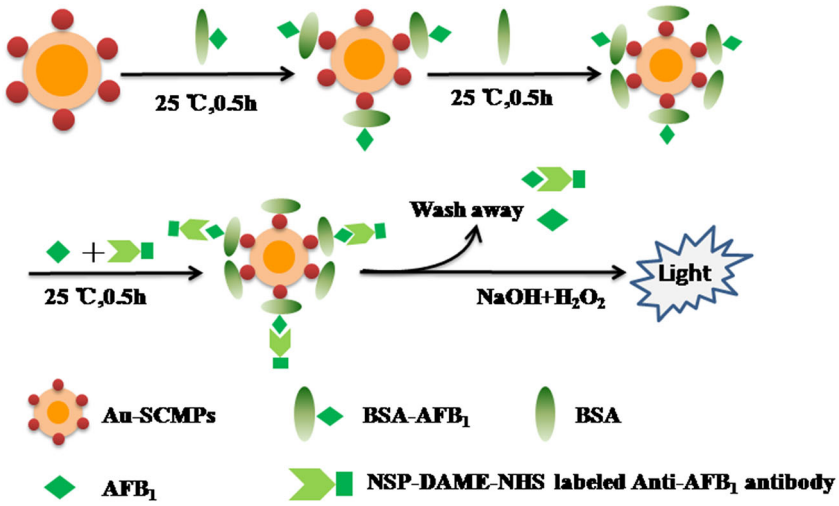

Fig. 1 The schematic principle of CL detection based on Au-SCMPs

Experimental

Materials

Aflatoxin B_1 (AFB_1), BSA-AFB_1 conjugate (BSA-AFB_1), and monoclonal antibody against AFB_1 (from mouse) (mAb-AFB_1) were purchased from Shandong Landu Biotechnology Company (Shandong China). 3-Aminopropyltrimethoxysilane (APTS) and bovine serum albumin (BSA) were purchased from J&K Scientific Co., Ltd (Beijing China). L-Lysine and Sephadex G-50 were purchased from Seebio (Shanghai, China). NSP-DMAE-NHS was purchased from MaterWin New Materials Co., Ltd (Shanghai, China). $FeCl_3 \cdot 6H_2O$, $HAuCl_4 \cdot 3H_2O$, tetraethoxysilane (TEOS), sodium acetate, sodium chloride, trisodium citrate, sodium phosphate monobasic (NaH_2PO_4), sodium phosphate dibasic (Na_2HPO4), methanol, ethanol, ethylene glycol, HCl, NaOH, and aqueous ammonia (28 wt. %) were of analytical grade and purchased from Tianjin Tianli Chemical Regents Ltd. Milk powder and dried peanuts were purchased from the local supermarket. All the chemicals were used without further treatment. Deionic water was used for all the experiments.

Synthesis of Fe_3O_4 Nanoparticles

Fe_3O_4 magnetic nanoparticles were prepared through a solvothermal method (Xu et al. 2006). Briefly, $FeCl_3 \cdot 6H_2O$ (1.89 g, 0.007 mol) and sodium acetate (5.04 g, 0.061 mol) were dissolved in 70 mL of ethylene glycol under vigorous stirring. The mixture was sealed in a Teflon-lined stainless-steel autoclave and maintained at 200 °C for 9 h. After the autoclave was cooled to room temperature (RT), the black products were washed several times with ethanol and dried in vacuum at 60 °C for 6 h.

Synthesis and Surface Modification of Fe_3O_4@SiO_2 Nanoparticles

The Fe_3O_4@SiO_2 nanoparticles were synthesized by a modified StÖber method (Deng et al. 2008). Typically, Fe_3O_4 nanoparticles (100 mg) were first treated with HCl aqueous solution (50 mL, 0.1 M) under ultrasonic vibration for 10 min. After that, the magnetic nanoparticles were washed with deionized water thoroughly, and then homogeneously dispersed in a mixture of ethanol (80 mL), deionized water (20 mL), and concentrated ammonia aqueous solution (1.0 mL, 28 wt.%). TEOS (0.023 g, 0.11 mol) was added to the solution and stirred for 8 h at RT. The product was separated by a magnet and washed with ethanol and water, then dried in vacuum at 60 °C for 10 h. For surface modification, the obtained Fe_3O_4@SiO_2 nanoparticles were redispersed in 150 mL ethanol, 1.5 mL ammonia aqueous solution (28 wt.%), and 0.75 mL APTS, and the mixture was stirred for 24 h (Rasch et al. 2009). The amine-functionalized nanoparticles were washed several times with ethanol and redispersed in 100 mL water, and then a few drops of concentrated HCl were added to maintained pH ~3.

Synthesis of Fe_3O_4@SiO_2@Au Nanoparticles

Gold colloids with different sizes (18, 30, and 50 nm) were prepared by reduction of $HAuCl_4$ with sodium citrate (Frens 1973). Then, 30 mL of the amine-functionalized Fe_3O_4@SiO_2 nanoparticles dispersion was added dropwise to 100 mL of the citrate-stabilized gold colloids. After about 1-h stirring, the resulting product was separated magnetically and washed with water.

Preparation of NSP-DAME-NHS-Labeled mAb-AFB_1 and BSA

The NSP-DAME-NHS-labeled mAb-AFB_1 and BSA were prepared according to Schlaeppi et al. (1994) but with some modifications. Purified mAb-AFB_1 (0.1 mg) dissolved in 320 μL of PBS (0.1 M, pH 8.0) was labeled by reacting with 28 μg of NSP-DAME-NHS for 1 h at RT. The reaction was quenched by adding 100 μL of l-lysine (10 mg mL^{-1} of H_2O) for 15 min. The labeled mAb-AFB_1 was separated from unbound NSP-DAME-NHS by gel filtration on a Sephadex G-50 column (1 × 25 cm) equilibrated with PBS (0.1 M, pH 7.4). The specific chemiluminescent activity of the labeled mAb-AFB_1 was estimated according to the absorbance at 280 nm and luminescent intensity. In addition, the NSP-DAME-NHS-labeled BSA was prepared using the same method.

Immobilization of BSA-AFB_1 on Au-SCMPs

The BSA-AFB_1 was immobilized on Au-SCMPs according to a modified procedure (Sung et al. 2013). Briefly, 50 μL of 20 mg mL^{-1} optimized Au-SCMPs was added to 60 μL of 0.02 mg mL^{-1} BSA-AFB_1 in PBS (0.1 M, pH 7.4) followed by gently shaking for 30 min at RT to induce the physical adsorption of the BSA-AFB_1 to Au colloids which is based on hydrophilic, hydrophobic, or both types of interactions (Jung et al. 2008). The supernatant of the mixture was discarded, and 120 μL of PBS (0.1 M, pH 7.4) containing 5 % BSA (*w*/*v*) was added to block the surface of the bare Au-SCMPs. The mixtures were incubated with shaking for 30 min at RT and separated by magnet. Subsequently, the Au-SCMPs were resuspended in 150 μL of PBS (0.1 M, pH 7.4) containing 0.1 % BSA (*w*/*v*) and shaken for 30 min at RT. The supernatant was discarded and resuspended in 150 μL of PBS (0.1 M, pH 7.4) containing 0.1 % BSA (*w*/*v*) again. The magnetic separation and resuspension was repeated twice, after which the resulting solution was stored at 4 °C before use.

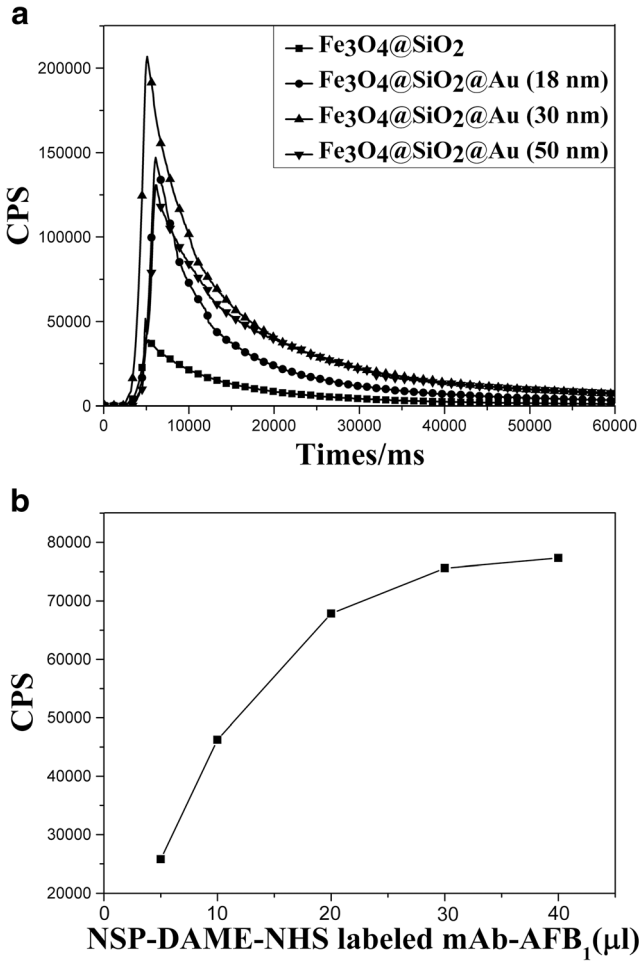

Fig. 2 **a** The CL intensity of different Au-SCMPs (Au 18, 30, and 50 nm) modified with NSP-DAME-NHS-labeled BSA. **b** The emission intensity versus the amount of NSP-DMAE-NHS-labeled mAb-AFB_1, of which the concentration was 0.01 mg mL^{-1}. Measurements were done in duplicate, and the average values were taken

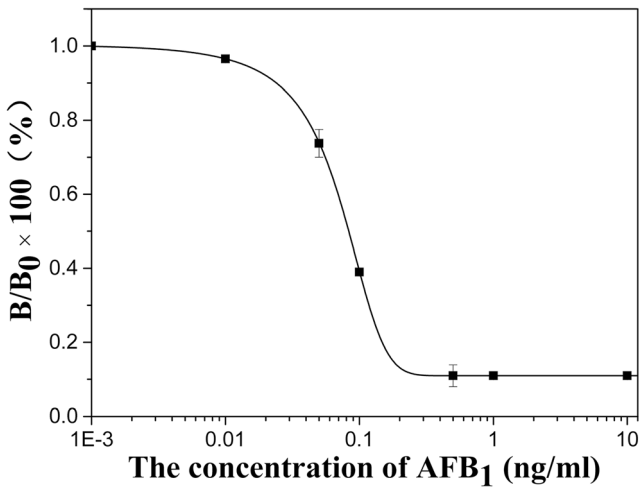

Fig. 3 Inhibition curve for the detection of AFB_1, where B/B_0 represents the percentage of NSP-DAME-NHS-labeled mAb-AFB_1 specifically bound to the nanoparticles

Competitive CL Assays for the AFB_1 Detection

Target analyte of AFB_1 was prepared by dissolving AFB_1 in a stock solution with PBS: methanol (9:1, *v*/*v*) (Xiulan et al. 2005). In a typical experiment, 1 mL of the target AFB_1 solutions (0.001, 0.01, 0.05, 0.1, 0.5, 1, and 10 ng mL^{-1}) were mixed with the optimized amount of labeled mAb-AFB_1 solution, respectively, and incubated for 30 min at RT. The BSA-AFB_1-immobilized Au-SCMPs were added, and the incubation was continued for another 30 min. The nanoparticles were washed four times with PBS in magnetic field and transferred into a CL measurement tube. Finally, the CL of the above nanoparticles was measured by a homemade luminescent measurement system (Fig. S1).

Method Validation

The method was validated for possible applications by analyzing real milk samples and ready-to-eat peanut samples. Milk samples for precision analysis were prepared as follows: 0.1 g of noninfected milk powder was dissolved in 1 mL distilled water by continuous stirring and spiked with different amounts of AFB_1. The sample was treated with equal volume methanol by shaking for 30 min and centrifuged at ~6000×*g* for 8 min at 4 °C. The upper fat layer was completely removed, and the aqueous layer (middle portion) was stored at 4 °C before use. For peanut samples, 1 g of ground blank peanut sample was spiked with different amounts of AFB_1 and then extracted with 5 mL methanol-water (7:3, *v*/*v*) by shaking for 30 min at RT. The suspension was filtered, and the filtrate was stored at 4 °C before use. The blank milk sample and peanut sample were prepared as described above but not spiked with AFB_1. The prepared milk samples and peanut samples were analyzed as analytes according to the competitive CL procedure ("Competitive CL Assays for the AFB_1 Detection").

Result and Discussion

Characterization of Fe_3O_4@SiO_2@Au Magnetic Nanoparticles

The phase structure and crystallization of the as-prepared nanoparticles were characterized by XRD analyses. FigureS2 shows the XRD patterns of (a) Fe_3O_4, (b) Fe_3O_4@SiO_2, and (c) Fe_3O_4@SiO_2@Au. The diffraction peaks in curve (a) match well with those of Fe_3O_4 from the JCPDS card (no. 75-0033) with a pure phase. After coating with the silica layer, a broad and weak peak (2θ, 25°) corresponding to the amorphous SiO_2 is appeared in curve (b). For the diffraction peaks in curve (c), two new peaks corresponding to the (111) and (200) planes of Au are clearly observed, indicating the grafting of Au colloids on the surface of Fe_3O_4@SiO_2 nanoparticles.

Table 1 Comparison of this method and other typical methods

Immunoassay method	LOD (ng mL^{-1})	IC_{50} (ng mL^{-1})	Reference
ELISA	0.05	0.62	Kolosova et al. (2006)
Fluoroimmunoassay	0.149	0.016	Zhang et al. (2014b)
Multiplex CL immunoassay	0.0019	0.01	Xu et al. (2014)
Enzyme immunoassay	2	10	Saha et al. (2007)
Electrochemical immunoassay	0.2	–	Masoomi et al. (2013)
Immunochromatography assay	2.5	–	Xiulan et al. (2006)
Improved CL immunoassay	0.01	0.07	This work

The morphology and size of nanoparticles were characterized by SEM and TEM. Figure S3 shows the SEM and TEM images for the nanoparticles obtained at different experimental stage. Figure S3a shows that the performed Fe_3O_4 templates are spherical in shape and have a mean diameter of about 300 nm. After coated with an amorphous silica layer, Fe_3O_4@SiO_2 nanoparticles with a thin silica ~20 nm were obtained (Fig. S3b). Figure S3f shows that Fe_3O_4@SiO_2 nanoparticles have an average particle size of 325 nm. Figure S3c–e shows the SEM images of Fe_3O_4@SiO_2@Au (18 nm), Fe_3O_4@SiO_2@Au (30 nm), and Fe_3O_4@SiO_2@Au (50 nm), respectively, indicating that the Au colloids with different size are successfully decorated on the Fe_3O_4@SiO_2 nanoparticles. However, large amounts of Au colloids (50 nm) aggregated in the sample of Fe_3O_4@SiO_2@Au (50 nm) which is consistent with previous report (Rasch et al. 2009; Zhang et al. 2014a).

Figure S4 shows the magnetic hysteresis loops of (a) Fe_3O_4, (b) Fe_3O_4@SiO_2, and (c) Fe_3O_4@SiO_2@Au nanoparticles which are characterized by a VSM apparatus at RT. As can be seen, the saturation magnetization values are 76.2, 73.7, and 64.6 emu g^{-1} for Fe_3O_4, Fe_3O_4@SiO_2, and Fe_3O_4@SiO_2@Au nanoparticles, respectively. The field-dependent magnetization shows very little hysteresis loop, indicating that the nanoparticles exhibit superparamagnetic behaviors. As a result, the nanoparticles in their homogeneous dispersion can be rapidly collected by a small magnet and redisperse quickly by gentle shaking once the magnet is removed. The as-prepared nanoparticles possess excellent magnetic responsivity and redispersibility which is greatly advantageous for CL immunoassays.

Optimization of the Au-SCMNPs

The relative CL intensity depends greatly on the amount of biomolecules by immobilization in competitive CL immunoassays. In this work, the capacity of different Au-SCMPs (18, 30, and 50 nm) in immobilization of BSA was investigated. Briefly, 50 μL of 20 mg mL^{-1} Au-SCMNPs (Au 18, 30, and 50 nm) was added to 60 μL of 0.1 mg mL^{-1} NSP-DAME-NHS-labeled BSA and shaken for 30 min at RT. After that, the Au-SCMPs were washed four times with PBS and the CL signal was measured. As shown in Fig. 2a, the most intensive CL signal was obtained for Fe_3O_4@SiO_2@Au (30 nm), indicating the most efficient in immobilization of BSA. Therefore, we chose Fe_3O_4@SiO_2@Au (30 nm) nanoparticles as BSA-AFB_1 immobilizing carrier in the following studies.

Determination of Optimized Amount of NSP-DAME-NHS-Labeled mAb-AFB_1

In order to improve the detection sensitivity, it is critical to determine the optimized amount of NSP-DAME-NHS-labeled mAb-AFB_1. Briefly, different amounts of NSP-DAME-NHS-labeled mAb-AFB_1 (5, 10, 20, 30, and 40 μL) with a concentration of 0.01 mg mL^{-1} were added to 50 μL of BSA-AFB_1 immobilized

Table 2 The results of the proposed CL immunoassay for milk and peanut samples

Sample	Expected concentration (ng mL^{-1})	Found concentration[a] (ng mL^{-1})	R.S.D.[b] (%)	Recovery (%)
Milk	0.1	0.107 ± 0.00846	7.9	107
	0.05	0.0466 ± 0.0056	12.1	93.3
	0.02	0.01924 ± 0.00055	2.9	96.2
Peanut	0.1	0.105 ± 0.00952	9.1	105
	0.05	0.0553 ± 0.00462	8.35	111
	0.02	0.0227 ± 0.00253	9.55	114

[a] The report data are the mean values ± SD

[b] Relative standard deviations (R.S.D.) of five determinations for each sample.

Au-SCMPs (20 mg mL^{-1}) and gently shaken for 30 min at RT. The particles were washed four times with PBS before CL emissions were measured. As shown in Fig. 2b, the CL intensity increased significantly versus the increase of NSP-DAME-NHS-labeled mAb-AFB_1 until 30 μL at which the CL intensity got saturation. Considering the sensor response and tracer consumption, we selected 30 μL of NSP-DAME-NHS-labeled mAb-AFB_1 in competitive immunoassay detections.

Calibration Curve and Sensitivity of the AFB_1 Detection

Figure 3 shows the calibration curve of the indirect competitive CL immunoassays using Fe_3O_4@SiO_2@Au (30 nm) as BSA-AFB_1 immobilizing carrier. The inhibition ratio has a good nonlinear relationship with the logarithm of AFB_1 concentration in the range of 0.01 to 0.2 ng mL^{-1}. The IC_{50} value was 0.07 ng mL^{-1} and the limit of detection (LOD) of AFB_1 was 0.01 ng mL^{-1}, respectively. Compared with other typical methods, the results in this work demonstrate an excellent sensitivity for the detection of AFB_1 (Table 1).

Sample Analysis

To investigate the accuracy and feasibility of the newly improved method for practical applications, several artificially spiked milk samples and peanut samples were analyzed. The blank sample and the control samples spiked with AFB_1 at 0.02, 0.05, and 0.1 ng mL^{-1} concentrations were prepared and testified. The analysis results were shown in Table 2. As can be seen from Table 2, the recoveries were between 93 and 114 %, demonstrating the applicability of the proposed method for the ultrasensitive detection of AFB_1 in real foods.

Conclusions

In this work, an improved CL immunoassay for the ultrasensitive detection of AFB_1 is described. In the proposed procedure, a new and efficient signal enhancer, NSP-DAME-NHS, and a simplified separation producer based on the optimized Au-SCMPs have been utilized to detect AFB_1. Results have shown that the IC_{50} value was 0.07 ng mL^{-1} and LOD of AFB_1 was 0.01 ng mL^{-1}, respectively. Compared to the conventional analytical assays, this method showed great potential for low-cost, rapid, and highly sensitive in the detection of AFB_1 in agricultural food and feed samples. This indirect competitive CL immunoassay is also suitable for detecting other small molecule analytes.

Compliance with Ethical Standards

Ethical approval This article does not contain any studies with human or animal subjects.

Informed Consent Not applicable

Funding This work was supported by the National Natural Science Foundation of China (NSFC, Grant No. 81371642) and the Fundamental Research Funds for the Central Universities of China (XKJC2013005).

Conflict of Interest Junfeng Li declares that he has no conflict of interest. Xiangyi Fang declares that he has no conflict of interest. Yucong Yang declares that she has no conflict of interest. Xiaoli Cheng declares that she has no conflict of interest. Peng Tang declares that he has no conflict of interest.

References

Ackerson CJ, Jadzinsky PD, Jensen GJ, Kornberg RD (2006) Rigid, specific, and discrete gold nanoparticle/antibody conjugates. J Am Chem Soc 128:2635–2640

Ahangaran F, Hassanzadeh A, Nouri S (2013) Surface modification of Fe_3O_4@SiO_2 microsphere by silane coupling agent. Int Nano Lett 3: 1–5

Bi S, Yan Y, Yang X, Zhang S (2009) Gold nanolabels for new enhanced chemiluminescence immunoassay of alpha-fetoprotein based on magnetic beads. Chem Eur J 15:4704–4709. doi:10.1002/chem.200801722

Blasco C, Picó Y (2011) Determining nanomaterials in food. Trac Trends Anal Chem 30:84–99

Bronstein I, Voyta JC, Thorpe GH, Kricka LJ, Armstrong G (1989) Chemiluminescent assay of alkaline phosphatase applied in an ultrasensitive enzyme immunoassay of thyrotropin. Clin Chem 35: 1441–1446

Castillo G, Poturnayova A, Snejdarkova M, Hianik T, Spinella K, Mosiello L Development of electrochemical aptasensor using dendrimers as an immobilization platform for detection of Aflatoxin B1 in food samples. In, 2015. IEEE, pp 1–4

Deng Y-H, Wang C-C, Hu J-H, Yang W-L, Fu S-K (2005) Investigation of formation of silica-coated magnetite nanoparticles via sol–gel approach. Colloids Surf A Physicochem Eng Asp 262:87–93

Deng Y, Qi D, Deng C, Zhang X, Zhao D (2008) Superparamagnetic high-magnetization microspheres with an Fe_3O_4@SiO_2 core and perpendicularly aligned mesoporous SiO_2 shell for removal of microcystins. J Am Chem Soc 130:28–29

Edelman RR, Warach S (1993) Magnetic resonance imaging. N Engl J Med 328:708–716

Frens G (1973) Controlled nucleation for the regulation of the particle size in monodisperse gold suspensions. Nature 241:20–22

Herzallah SM (2009) Determination of aflatoxins in eggs, milk, meat and meat products using HPLC fluorescent and UV detectors. Food Chem 114:1141–1146

Hui C et al (2011) Core-shell Fe_3O_4@SiO_2 nanoparticles synthesized with well-dispersed hydrophilic Fe_3O_4 seeds. Nanoscale 3:701–705

Iranifam M, Fathinia M, Sadeghi Rad T, Hanifehpour Y, Khataee AR, Joo SW (2013) A novel selenium nanoparticles-enhanced chemiluminescence system for determination of dinitrobutylphenol. Talanta 107:263–269. doi:10.1016/j.talanta.2012.12.043

Jung Y, Jeong JY, Chung BH (2008) Recent advances in immobilization methods of antibodies on solid supports. Analyst 133:697–701

Kolosova AY, Shim W-B, Yang Z-Y, Eremin SA, Chung D-H (2006) Direct competitive ELISA based on a monoclonal antibody for detection of aflatoxin B1. Stabilization of ELISA kit components and application to grain samples. Anal Bioanal Chem 384:286–294

Korde A et al (2003) Development of a radioimmunoassay procedure for aflatoxin B1 measurement. J Agric Food Chem 51:843–846

Lim IIS, Mott D, Ip W, Njoki PN, Pan Y, Zhou S, Zhong C-J (2008) Interparticle interactions in glutathione mediated assembly of gold nanoparticles. Langmuir 24:8857–8863

Masoomi L, Sadeghi O, Banitaba MH, Shahrjerdi A, Davarani SSH (2013) A non-enzymatic nanomagnetic electro-immunosensor for determination of Aflatoxin B1 as a model antigen. Sensors Actuators B Chem 177:1122–1127

Mervartová K, Polášek M, Calatayud JM (2007) Recent applications of flow-injection and sequential-injection analysis techniques to chemiluminescence determination of pharmaceuticals. J Pharm Biomed Anal 45:367–381

Mojić B, Giannakopoulos KP, Cvejić Ž, Srdić VV (2012) Silica coated ferrite nanoparticles: Influence of citrate functionalization procedure on final particle morphology. Ceram Int 38:6635–6641

Navas MJ, Jimenez AM (1996) Review of chemiluminescent methods in food analysis. Food Chem 55:7–15

Pankhurst QA, Connolly J, Jones SK, Dobson JJ (2003) Applications of magnetic nanoparticles in biomedicine. J Phys D Appl Phys 36: R167

Pingarrón JM, Yanez-Sedeno P, González-Cortés A (2008) Gold nanoparticle-based electrochemical biosensors. Electrochim Acta 53:5848–5866

Rasch MR, Sokolov KV, Korgel BA (2009) Limitations on the optical tunability of small diameter gold nanoshells. Langmuir 25:11777–11785

Ren M et al (2014) Immunochromatographic assay for ultrasensitive detection of aflatoxin B1 in maize by highly luminescent quantum dot beads. ACS Appl Mater Interfaces 6:14215–14222

Saha D, Acharya D, Roy D, Shrestha D, Dhar TK (2007) Simultaneous enzyme immunoassay for the screening of aflatoxin B1 and ochratoxin A in chili samples. Anal Chim Acta 584:343–349

Schlaeppi J-MA, Kessler A, Foery W (1994) Development of a magnetic particle-based automated chemiluminescent immunoassay for triasulfuron. J Agric Food Chem 42:1914–1919

Sorouraddin MH, Iranifam M, Imani-Nabiyyi A (2008) A novel captopril chemiluminescence system for determination of copper(II) in human hair and cereal flours. J Fluoresc 19:575–581. doi:10.1007/s10895-008-0447-6

Sung YJ, Suk H-J, Sung HY, Li T, Poo H, Kim M-G (2013) Novel antibody/gold nanoparticle/magnetic nanoparticle nanocomposites for immunomagnetic separation and rapid colorimetric detection of Staphylococcus aureus in milk. Biosens Bioelectron 43:432–439

Xiulan S, Xiaolian Z, Jian T, Zhou J, Chu FS (2005) Preparation of gold-labeled antibody probe and its use in immunochromatography assay for detection of aflatoxin B1. Int J Food Microbiol 99:185–194

Xiulan S, Xiaolian Z, Jian T, Xiaohong G, Jun Z, Chu FS (2006) Development of an immunochromatographic assay for detection of aflatoxin B1 in foods. Food Control 17:256–262

Xu X, Deng C, Gao M, Yu W, Yang P, Zhang X (2006) Synthesis of magnetic microspheres with immobilized metal ions for enrichment and direct determination of phosphopeptides by matrix-assisted laser desorption ionization mass spectrometry. Adv Mater 18:3289–3293

Xu K et al (2014) Multiplex chemiluminescent immunoassay for screening of mycotoxins using photonic crystal microsphere suspension array. Analyst 139:771–777

Yang X-Y, Guo Y-S, Bi S, Zhang S-S (2009) Ultrasensitive enhanced chemiluminescence enzyme immunoassay for the determination of α-fetoprotein amplified by double-codified gold nanoparticles labels. Biosens Bioelectron 24:2707–2711. doi:10.1016/j.bios.2008.12.009

Zhang J, Qi H, Li Y, Yang J, Gao Q, Zhang C (2008) Electrogenerated chemiluminescence DNA biosensor based on hairpin DNA probe labeled with ruthenium complex. Anal Chem 80:2888–2894

Zhang D et al (2010) Carbon-stabilized iron nanoparticles for environmental remediation. Nanoscale 2:917–919

Zhang X, Zhu Y, Yang X, Zhou Y, Yao Y, Li C (2014a) Multifunctional Fe_3O_4@TiO_2@Au magnetic microspheres as recyclable substrates for surface-enhanced Raman scattering. Nanoscale 6:5971–5979

Zhang Z, Li Y, Li P, Zhang Q, Zhang W, Hu X, Ding X (2014b) Monoclonal antibody-quantum dots CdTe conjugate-based fluoroimmunoassay for the determination of aflatoxin B1 in peanuts. Food Chem 146:314–319